

Localizations of the septin Spn4 tagged with GFP and mEGFP in fission yeast

Jack R. Gregory^{1,2,3}, Nicholas J. Ricottilli¹, Jian-Qiu Wu^{1§}

Abstract

Septins are cytoskeletal proteins crucial for cell division and many other processes. In fission yeast, septins localize to the division site during septum formation. Recently, we conducted a study that elucidates the localizations and functionalities of epitope-tagged septins. However, some questions remain outstanding. Here we assessed the impacts of monomeric mEGFP and dimeric GFP(S65T) on the septin Spn4 tagged at either of its terminus. We found that septin levels were important for its function, Spn4-mEGFP localized normally to the division site, but GFP(S65T)-Spn4 formed elongated structures ectopically, further highlighting that dimeric tags are more disruptive to septin localizations.

¹Department of Molecular Genetics, The Ohio State University, Columbus, Ohio, United States

²Molecular, Cellular, and Developmental Biology Graduate Program, The Ohio State University, Columbus, Ohio, United States

³Cellular, Molecular, and Biochemical Sciences Program, The Ohio State University, Columbus, Ohio, United States

[§]To whom correspondence should be addressed: wu.620@osu.edu

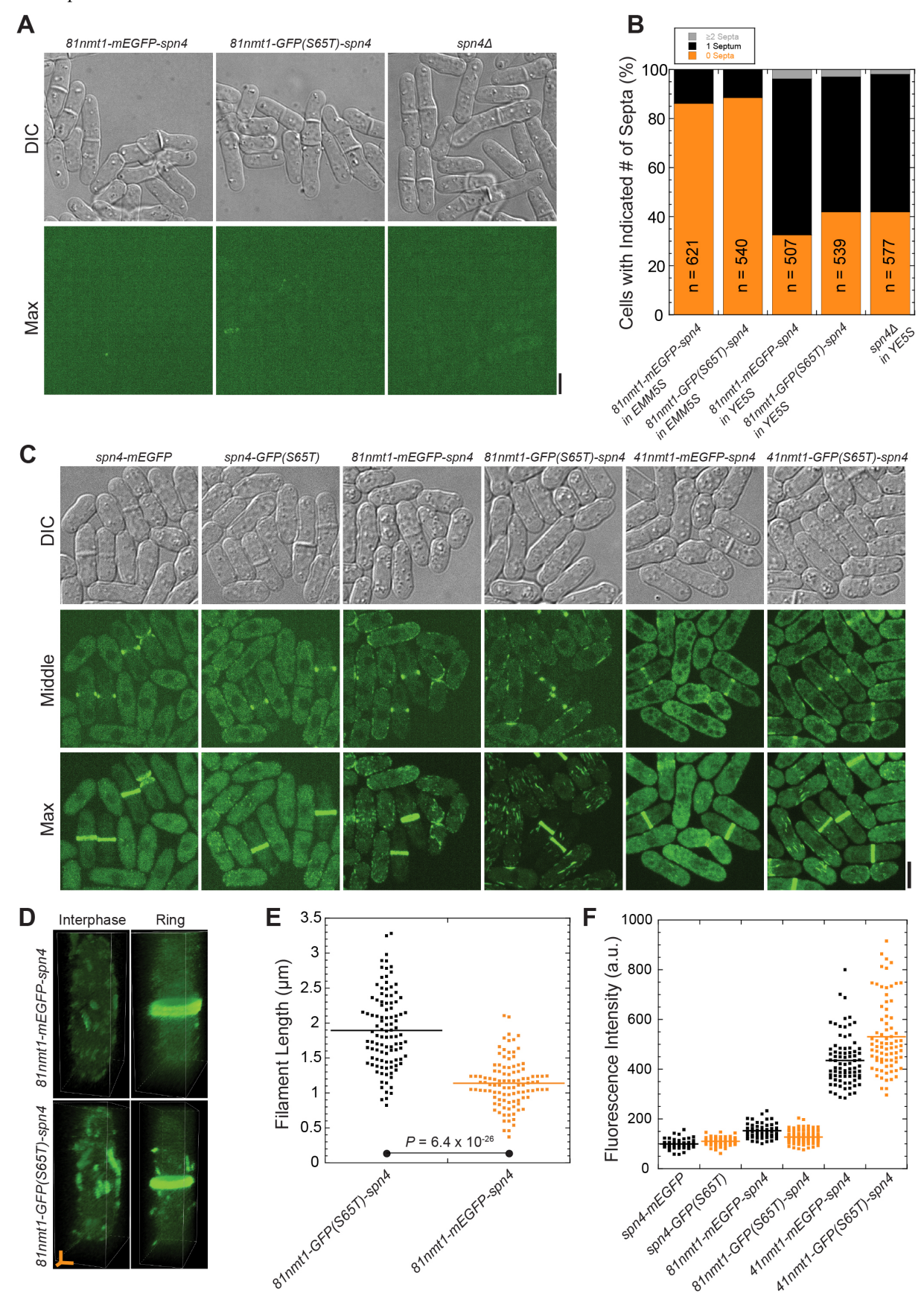


Figure 1. The localization of the septin Spn4 and morphology of the strains expressing Spn4 tagged with mEGFP or GFP(S65T) at either N or C-terminus:

(A and B) Spn4 depletion leads to septation defects. Cells were grown in YE5S and diluted as needed to ensure exponential growth for \sim 36 h before imaging on a YE5S + gelatin pad. (A) Cell morphology from Differential Image Contrast (DIC) and the signal of Spn4 showing the maximal intensity projection of 25 slices with 0.3 μ m spacing. (B)



Quantification of the number of septa per cell from DIC images of the indicated strains. (C-F) Localization and quantification of Spn4 (filament lengths and protein levels) in the indicated strains. The indicated strains were grown in YE5S for ~12 h. Then, they were washed 3x with EMM5S and grown exponentially in EMM5S for ~24 h before imaging on an EMM5S + gelatin pad. (C) Cell morphology and the localization of Spn4 are shown via DIC, fluorescence images at the middle focal plane and the maximal intensity projection of 25 slices with 0.3 μ m spacing. (D) 3D volumetric projections of 81nmt-mEGFP-spn4 and 81nmt1-GFP(S65T)-spn4 are shown for cells in interphase and during cytokinesis (Ring). (E) The three longest Spn4 filaments (excluding the septin rings) from each cell were measured. n = 105 filaments for each strain. (F) The mean Spn4 fluorescence intensity in the indicated strains after subtraction of the mean background intensity in $spn4\Delta$ cells. $n \ge 50$ cells for each strain. Scale bars, 5 μ m. Axial bars, 2 μ m.

Description

The septin family of proteins was named after their critical functions for septum formation during cytokinesis in dividing yeast cells (Ford & Pringle, 1991; Haarer & Pringle, 1987; Hartwell, 1971; Kim et al., 1991). In budding yeast, septins first form as a nascent ring at the bud emergence and then form an hourglass with both longitudinal and latitudinal filaments; these filaments transition into a double ring during cytokinesis, before dissociating from the division site after the daughter cells separate (Byers & Goetsch, 1976; Chant et al., 1995; Marquardt et al., 2019, 2021; Rodal et al., 2005; Varela Salgado & Piatti, 2024). Septins act as an essential scaffold for the myosin-II ring and other proteins at the bud neck for cytokinesis and other processes (Bi et al., 1998; Gladfelter et al., 2001; Hartwell, 1971; Takizawa et al., 2000). In other model organisms, the septins also serve as scaffolds and/or diffusion barriers and play crucial roles in many cellular processes such as cytokinesis, plasma membrane repair, gamete formation, exocytosis, neuronal development, and others (Fares et al., 1995; Gladfelter, 2006; Kinoshita et al., 1997; Kwitny et al., 2010; Onishi et al., 2010; Prislusky et al., 2024; Singh et al., 2025; Tasto et al., 2003).

The septins accomplish these numerous functions by forming palindromic heterooligomers (An et al., 2004; Bertin et al., 2008; Cavini et al., 2021). In most species, the septins form hexamers or octamers, which are the basic building block for higher-order structures, composed of two units of each septin protein. The septins interact via their two faces— the G and NC faces— forming G to G or NC to NC interactions (Sirajuddin et al., 2007). When forming the oligomers, the C terminal tails of septins stick out from the complex (Cavini et al., 2021; Sirajuddin et al., 2007). Once formed, the oligomers then polymerize into filaments that can assemble into rings, hourglass, gauzes, meshes, bars, fibers, patches, and other structures in the cell (Bridges et al., 2014; Byers & Goetsch, 1976; Garcia et al., 2011; Hernández-Rodríguez et al., 2012; Rodal et al., 2005; Vrabioiu & Mitchison, 2006).

The fission yeast *Schizosaccharomyces pombe* is an attractive genetically tractable model organism to study septins and other fundamental cellular processes (Fantes & Hoffman, 2016; Hoffman et al., 2015; Pollard & Wu, 2010). In *S. pombe*, four septins are involved in cytokinesis, septum formation, and daughter-cell separation: Spn1, Spn3, and Spn4 (An et al., 2004; Berlin et al., 2003; Longtine et al., 1996; Tasto et al., 2003). The organization of the septins at the division site is regulated by the anillin-like protein Mid2, while the actomyosin contractile ring is regulated by the other anillin-like protein, Mid1 (Arbizzani et al., 2022; Bähler, et al., 1998; Berlin et al., 2003; Hachet & Simanis, 2008; Lee & Wu, 2012; Petit et al., 2005; Saha & Pollard, 2012; Sohrmann et al., 1996; Tasto et al., 2003). The four septins localize to the division site as unconstricted double rings on both sides of the contractile ring during cytokinesis and septum formation (An et al., 2004; Berlin et al., 2003; Longtine et al., 1996; Tasto et al., 2003; Wu et al., 2003). They are crucial for the localizations of Rho4 GTPase, Rho guanine nucleotide exchange factor Gef3, and the exocyst to the division site (Muñoz et al., 2014; Singh et al., 2025; Wang et al., 2015).

We recently reported that the localization and function of septins are susceptible to epitope tagging (Gregory et al., 2025). We found that the septins Spn1 and Spn4 expressed under their native promoters have dramatically distinct localizations on the plasma membrane with different fluorescence tags. The septins Spn1 and Spn4 tagged with tdTomato and 3HA are less functional or not functional at all, which results in localization artifacts on the plasma membrane or a loss of septin localization and function (Gregory et al., 2025). By contrast, the septins tagged with mEGFP and mYFP are more functional and localize normally to the division site (Gregory et al., 2025). Our results emphasize the need to rigorously test the functionality of epitope-tagged septins and other proteins. However, several questions were left unanswered. First, no mEGFP tagged Spn4 strains were available for comparison with GFP(S65T) tagged strains (Gregory et al., 2025), which left us uncertain if the Spn4 localization we observed was caused by weak dimeric GFP(S65T) or not (Oltrogge et al., 2014). Second, how the expression level of a single septin affects the overall septin localization and function remains unclear in fission yeast.

We first tagged $\underline{Spn4}$ with mEGFP at its C-terminus under its native promoter and at its N-terminus with the 41nmt1 (medium strength) and 81nmt1 (weak) promoters using PCR-based gene targeting (Bähler, et al., 1998). The nmt1 promoters are induced in medium without thiamine and repressed with thiamine (Basi et al., 1993; Maundrell, 1990). A previous study has reported that cells depleted of both $\underline{Spn1}$ and $\underline{Spn4}$ in the 81nmt1- $\underline{spn1}$ 81nmt1- $\underline{spn4}$ strain resemble $spn1\Delta$ or $spn4\Delta$ cells (Wu et al., 2010). We found that 81nmt1-mEGFP- $\underline{spn4}$ and 81nmt1-GFP(S65T)- $\underline{spn4}$ cells grown in YE5S liquid media (with unknown amount of thiamine from yeast extract) resembled $spn4\Delta$ in cell morphology and



septation index (Figure 1A-B). Consistently, <u>Spn4</u> signal was barely visible in these cells (Figure 1A). Thus, low amounts of <u>Spn4</u> are not sufficient for normal septin localization and function.

Next, we compared the <u>Spn4</u> localization (tagged with GFP[S65T] vs. mEGFP) and cell morphology in *81nmt1* (inducing condition), *41nmt1* (inducing condition), and C-terminally tagged <u>spn4</u> strains using confocal microscopy (Figure 1C-F). Overall, the mEGFP-tagged strains that expressed <u>Spn4</u> at different levels showed no or much less <u>Spn4</u> structures on the plasma membrane or in the cytoplasm outside the septin double rings and were less likely to form elongated structures than GFP(S65T)-tagged strains (Figure 1C-F). Interestingly, N-terminally tagged <u>Spn4</u> seemed more likely to form additional structures besides the rings, whereas Spn4-mEGFP appeared only in the rings at the division site as previously reported for the more functional septin-fusion proteins (An et al., 2004; Gregory et al., 2025). Moreover, all the strains resembled the wild type in cell morphology and septation index (Figure 1B-C).

To compare the differences between N-terminally mEGFP and GFP(S65T) tagged Spn4 strains in more detail, we observed the 3D volumetric projections of the 81nmt1 strains grown under inducing conditions (Figure 1D), which expressed at levels close (slightly higher) to the C-terminally tagged Spn4 (Figure 1F). The mEGFP-tagged strain had fewer elongated structures. In contrast, the GFP(S65T)-tagged strain had many long filaments, which even persisted after the septin rings had formed at the division site (Figure 1D). Indeed, quantification of the three longest Spn4 structures (not counting the septin rings) in each cell revealed that 81nmt1-GFP(S65T)-spn4 cells had significantly longer Spn4 structures (Figure 1E). In time-lapse microscopy, the elongated structures more likely moved or flowed longer distances at a higher velocity in 81nmt1-GFP(S65T)-spn4 than in 81nmt1-mEGFP-spn4 cells, which suggest that they are likely not associated with the plasma membrane (Extended Data). These structures were reminiscent of the septin fibers or bars that we and other labs observed previously (Davidson et al., 2016; DeMay et al., 2010; Gregory et al., 2025). It is unlikely these different Spn4 structures are due to varied Spn4 protein levels because the quantification of the mean fluorescence intensity revealed that Spn4 levels under the 81nmt1 promoter (inducing condition) were within a factor of two compared to Spn4 under its native promoter (Figure 1F). Moreover, in 41nmt1-GFP(S65T)-spn4 but not in 41nmt1-mEGFP-spn4 cells, <u>Spn4</u> formed similar elongated structures as in 81nmt1-GFP(S65T)-<u>spn4</u> cells, despite the <u>Spn4</u> levels being ~3-5 times higher (Figure 1F). Collectively, these structures, likely artefacts caused by the non-monomeric fluorophore, reveal the range of possible structures that Spn4, and by implication the septin proteins, can form when perturbed. It is important to note the impact of epitope tagging on Spn4 in particular because alongside Spn1, Spn4 forms the core of the septin octamer in fission yeast (An et al., 2004). Spn4 and Spn1 are essential for septin polymerization, and perturbations to these septins may disrupt the formation of the septin complex (An et al., 2004; Gregory et al., 2025).

In conclusion, our study reveals that minimal levels of the septin <u>Spn4</u> are important for septin localization and function. We find that non-monomeric GFP(S65T) tagged <u>Spn4</u> is more likely to form ectopic structures outside the septin rings. We also show that both ends of <u>Spn4</u> are susceptible to perturbations by an epitope tag, the N-terminus being more easily perturbed. Caution and careful assessments are required when seeking to understand any potentially novel structures formed by the septins.

Methods

Strains constructed and used in this study are listed in Table 1. We carried out gene targeting to tag Spn4 using the PCRbased homologous recombination method as previously described (Bähler, et al., 1998; Rutherford et al., 2024). The Cterminally tagged strains were controlled by the <u>spn4</u> native promoter with the *ADH1* terminator. For N-terminal tagged strains, the nmt1 promoters and encoding sequences for mEGFP or GFP(S65T) were inserted before the start codon of <u>spn4</u> and the <u>spn4</u> terminator was used. Growth (at 25°C), preparation, and imaging of fission yeast strains were done as previously described (Davidson et al., 2015; Gregory et al., 2025; Singh et al., 2025; Ye et al., 2025; Zhang et al., 2025). Briefly, each strain was woken up from the -80°C stocks onto YE5S plates. For strains grown in EMM5S minimal medium, strains were first grown in YE5S rich liquid medium for ~12 h, then washed 3x with EMM5S by spinning down the cells at 3,000 rpm for 30 sec and resuspending in EMM5S. The cells were then grown exponentially for ~24 h before being imaged on EMM5S + 20% gelatin pads (Davidson et al., 2016). For strains grown and imaged in YE5S, strains were grown exponentially in YE5S for ~36 h, and diluted twice a day to keep the cells in log phase of growth. Then, they were imaged on YE5S + 20% gelatin pads, after being collected by centrifugation at 3,000 rpm for 30 sec. To protect the cells from free radicals during imaging, n-propyl gallate (PG) was used at a final concentration of 5 µM. We imaged the cells at ~23°C on a Nikon CSU-W1 SoRa spinning disk confocal microscope with Hamamatsu ORCA Quest qCMOS camera C15550 on Nikon Eclipse Ti2 microscope with Plan Apo λD 100x/1.45 numerical aperture (NA) oil objective. Both mEGFP and GFP(S65T) fluorescently tagged proteins were imaged with a 488 nm laser at 30% power for single Z stacks and 20% power for movies.

All image analyses were done on either NIS elements or Fiji as previously described (Davidson et al., 2016; Gregory et al., 2025; Longo et al., 2022; Singh et al., 2025; Ye et al., 2025). Filament length was measured by drawing a line in Fiji along the length of the three longest filaments in individual cells. Fluorescence intensity was measured by drawing an ROI around the periphery of individual cells to measure the mean intensity. The intensities for all the measured cells were corrected for the background by subtracting the mean intensity from $50 \text{ spn}4\Delta$ cells. The brightness difference between



mEGFP and GFP(S65T) was corrected by dividing the GFP(S65T) values by 0.91, which is the conversion rate calculated from each fluorophore's extinction coefficient and quantum yield (Cranfill et al., 2016; Patterson et al., 1997). The *p* value was calculated using unpaired two-tailed Student's t-test.

Reagents

Strain name	Genotype	Figure/Movie
JW81	h- ade6-210 ura4-D18 leu1-32	For gene targeting
JW295	h+ spn4∆::kanMX6 leu1-32 ura4-D18	Figure 1A, B, F
JW10492	h- spn4-mEGFP:kanMX6 ade6-M210 leu1-32 ura4-D18	Figure 1C, F
JW8589	spn4-GFP(S65T):kanMX6 ade6 leu1-32 ura4-D18	Figure 1C, F
JW10461	h- kanMX6:81nmt1-mEGFP- <u>spn4</u> ade6-210 ura4-D18 leu1-32	Figure 1A-F; Movie 1
JW311	h- kanMX6:81nmt1-GFP(S65T)- <u>spn4</u> ade6-M210 leu1-32 ura4-D18	Figure 1A-F; Movie 1
JW10474	h- kanMX6:41nmt1-mEGFP- <u>spn4</u> ade6-210 ura4-D18 leu1-32	Figure 1C, F
JW310	h- kanMX6:41nmt1-GFP(S65T)- <u>spn4</u> ade6-M210 leu1-32 ura4-D18	Figure 1C, F
Plasmid name		
JQW75	pFA6a-kanMX6-P41nmt1-mEGFP	
JQW78	pFA6a-kanMX6-P81nmt1-mEGFP	
JQW85	pFA6a-mEGFP-kanMX6	

Acknowledgements: We are grateful to PomBase for providing and maintaining the indispensable fission yeast database. We would like to thank John Pringle and former members of the Wu lab for fission yeast strains and current members of the Wu lab for helpful discussion and technical support.

Extended Data

Description: Movie 1. Time-lapse microscopy of the septin Spn4 in 81nmt1-mEGFP-spn4 and 81nmt1-GFP(S65T)-spn4 strains. The indicated strains were grown in YE5S for ~12 h, and then were washed 3x with EMM5S and grown exponentially in EMM5S for ~24 h at 25°C. These strains were imaged on an EMM5S + gelatin pad using a spinning disk confocal microscope every 30 sec for 1 h. Maximal intensity projection of 5 slices with 2 μm spacing are shown. 7 frames per second.. Resource Type: Audiovisual. File: Movie 1.mp4. DOI: 10.22002/e4bh4-a6g30

References

An H, Morrell JL, Jennings JL, Link AJ, Gould KL. 2004. Requirements of fission yeast septins for complex formation, localization, and function. Mol Biol Cell 15(12): 5551-64. PubMed ID: <u>15385632</u>

Arbizzani F, Mavrakis M, Hoya M, Ribas JC, Brasselet S, Paoletti A, Rincon SA. 2022. Septin filament compaction into rings requires the anillin Mid2 and contractile ring constriction. Cell Rep 39(3): 110722. PubMed ID: 35443188

Bähler J, Steever AB, Wheatley S, Wang YL, Pringle JR, Gould KL, McCollum D. 1998. Role of polo kinase and Mid1p in determining the site of cell division in fission yeast. J Cell Biol 143(6): 1603-16. PubMed ID: 9852154

Bähler J, Wu JQ, Longtine MS, Shah NG, McKenzie A III, Steever AB, et al., Pringle JR. 1998. Heterologous modules for efficient and versatile PCR-based gene targeting in *Schizosaccharomyces pombe*. Yeast 14(10): 943-51. PubMed ID: 9717240



Basi G, Schmid E, Maundrell K. 1993. TATA box mutations in the *Schizosaccharomyces pombe nmt1* promoter affect transcription efficiency but not the transcription start point or thiamine repressibility. Gene 123(1): 131-6. PubMed ID: 8422997

Berlin A, Paoletti A, Chang F. 2003. Mid2p stabilizes septin rings during cytokinesis in fission yeast. J Cell Biol 160(7): 1083-92. PubMed ID: <u>12654901</u>

Bertin A, McMurray MA, Grob P, Park SS, Garcia G III, Patanwala I, et al., Nogales E. 2008. *Saccharomyces cerevisiae* septins: supramolecular organization of heterooligomers and the mechanism of filament assembly. Proc Natl Acad Sci U S A 105(24): 8274-9. PubMed ID: <u>18550837</u>

Bi E, Maddox P, Lew DJ, Salmon ED, McMillan JN, Yeh E, Pringle JR. 1998. Involvement of an actomyosin contractile ring in *Saccharomyces cerevisiae* cytokinesis. J Cell Biol 142(5): 1301-12. PubMed ID: <u>9732290</u>

Bridges AA, Zhang H, Mehta SB, Occhipinti P, Tani T, Gladfelter AS. 2014. Septin assemblies form by diffusion-driven annealing on membranes. Proc Natl Acad Sci U S A 111(6): 2146-51. PubMed ID: <u>24469790</u>

Byers B, Goetsch L. 1976. A highly ordered ring of membrane-associated filaments in budding yeast. J Cell Biol 69(3): 717-21. PubMed ID: 773946

Cavini IA, Leonardo DA, Rosa HVD, Castro DKSV, D'Muniz Pereira H, Valadares NF, Araujo APU, Garratt RC. 2021. The structural biology of septins and their filaments: an update. Front Cell Dev Biol 9: 765085. PubMed ID: 34869357

Chant J, Mischke M, Mitchell E, Herskowitz I, Pringle JR. 1995. Role of Bud3p in producing the axial budding pattern of yeast. J Cell Biol 129(3): 767-78. PubMed ID: 7730410

Cranfill PJ, Sell BR, Baird MA, Allen JR, Lavagnino Z, de Gruiter HM, et al., Piston DW. 2016. Quantitative assessment of fluorescent proteins. Nat Methods 13(7): 557-62. PubMed ID: <u>27240257</u>

Davidson R, Laporte D, Wu JQ. 2015. Regulation of Rho-GEF Rgf3 by the arrestin Art1 in fission yeast cytokinesis. Mol Biol Cell 26(3): 453-66. PubMed ID: <u>25473118</u>

Davidson R, Liu Y, Gerien KS, Wu JQ. 2016. Real-time visualization and quantification of contractile ring proteins in single living cells. Methods Mol Biol 1369: 9-23. PubMed ID: 26519302

DeMay BS, Meseroll RA, Occhipinti P, Gladfelter AS. 2010. Cellular requirements for the small molecule forchlorfenuron to stabilize the septin cytoskeleton. Cytoskeleton (Hoboken) 67(6): 383-99. PubMed ID: 20517926

Fantes PA, Hoffman CS. 2016. A brief history of *Schizosaccharomyces pombe* research: a perspective over the past 70 years. Genetics 203(2): 621-9. PubMed ID: 27270696

Fares H, Peifer M, Pringle JR. 1995. Localization and possible functions of *Drosophila* septins. Mol Biol Cell 6(12): 1843-59. PubMed ID: 8590810

Ford SK, Pringle JR. 1991. Cellular morphogenesis in the *Saccharomyces cerevisiae* cell cycle: localization of the *CDC11* gene product and the timing of events at the budding site. Dev Genet 12(4): 281-92. PubMed ID: 1934633

Garcia G III, Bertin A, Li Z, Song Y, McMurray MA, Thorner J, Nogales E. 2011. Subunit-dependent modulation of septin assembly: budding yeast septin Shs1 promotes ring and gauze formation. J Cell Biol 195(6): 993-1004. PubMed ID: 22144691

Gladfelter AS, Pringle JR, Lew DJ. 2001. The septin cortex at the yeast mother-bud neck. Curr Opin Microbiol 4(6): 681-9. PubMed ID: <u>11731320</u>

Gladfelter AS. 2006. Control of filamentous fungal cell shape by septins and formins. Nat Rev Microbiol 4(3): 223-9. PubMed ID: <u>16429163</u>

Gregory JR, Llaneza IMA, Osmani AH, Gosselin HE, Sabzian SA, Wu JQ. 2025. Localization and function of septins are susceptible to epitope tagging. Mol Biol Cell 36(12):ar148. PubMed ID: 41091578

Haarer BK, Pringle JR. 1987. Immunofluorescence localization of the *Saccharomyces cerevisiae CDC12* gene product to the vicinity of the 10-nm filaments in the mother-bud neck. Mol Cell Biol 7(10): 3678-87. PubMed ID: 3316985

Hachet O, Simanis V. 2008. Mid1p/anillin and the septation initiation network orchestrate contractile ring assembly for cytokinesis. Genes Dev 22(22): 3205-16. PubMed ID: 19056897

Hartwell LH. 1971. Genetic control of the cell division cycle in yeast: IV. Genes controlling bud emergence and cytokinesis. Exp Cell Res 69(2): 265-76. PubMed ID: 4950437

Hernández-Rodríguez Y, Hastings S, Momany M. 2012. The septin AspB in *Aspergillus nidulans* forms bars and filaments and plays roles in growth emergence and conidiation. Eukaryot Cell 11(3): 311-23. PubMed ID: <u>22247265</u>



Hoffman CS, Wood V, Fantes PA. 2015. An ancient yeast for young geneticists: a primer on the *Schizosaccharomyces pombe* model system. Genetics 201(2): 403-23. PubMed ID: <u>26447128</u>

Kim HB, Haarer BK, Pringle JR. 1991. Cellular morphogenesis in the *Saccharomyces cerevisiae* cell cycle: localization of the *CDC*3 gene product and the timing of events at the budding site. J Cell Biol 112(4): 535-44. PubMed ID: 1993729

Kinoshita M, Kumar S, Mizoguchi A, Ide C, Kinoshita A, Haraguchi T, Hiraoka Y, Noda M. 1997. Nedd5, a mammalian septin, is a novel cytoskeletal component interacting with actin-based structures. Genes Dev 11(12): 1535-47. PubMed ID: 9203580

Kwitny S, Klaus AV, Hunnicutt GR. 2010. The annulus of the mouse sperm tail is required to establish a membrane diffusion barrier that is engaged during the late steps of spermiogenesis. Biol Reprod 82(4): 669-78. PubMed ID: 20042538

Lee IJ, Wu JQ. 2012. Characterization of Mid1 domains for targeting and scaffolding in fission yeast cytokinesis. J Cell Sci 125(Pt 12): 2973-85. PubMed ID: <u>22427686</u>

Longo LVG, Goodyear EG, Zhang S, Kudryashova E, Wu JQ. 2022. Involvement of Smi1 in cell wall integrity and glucan synthase Bgs4 localization during fission yeast cytokinesis. Mol Biol Cell 33(2): ar17. PubMed ID: <u>34910579</u>

Longtine MS, DeMarini DJ, Valencik ML, Al-Awar OS, Fares H, De Virgilio C, Pringle JR. 1996. The septins: roles in cytokinesis and other processes. Curr Opin Cell Biol 8(1): 106-19. PubMed ID: 8791410

Marquardt J, Chen X, Bi E. 2019. Architecture, remodeling, and functions of the septin cytoskeleton. Cytoskeleton (Hoboken) 76(1): 7-14. PubMed ID: <u>29979831</u>

Marquardt J, Chen X, Bi E. 2021. Septin assembly and remodeling at the cell division site during the cell cycle. Front Cell Dev Biol 9: 793920. PubMed ID: 34901034

Maundrell K. 1990. *nmt1* of fission yeast. A highly transcribed gene completely repressed by thiamine. J Biol Chem 265(19): 10857-64. PubMed ID: <u>2358444</u>

Muñoz S, Manjón E, Sánchez Y. 2014. The putative exchange factor Gef3p interacts with Rho3p GTPase and the septin ring during cytokinesis in fission yeast. J Biol Chem 289(32): 21995-2007. PubMed ID: 24947517

Oltrogge LM, Wang Q, Boxer SG. 2014. Ground-state proton transfer kinetics in green fluorescent protein. Biochemistry 53(37): 5947-57. PubMed ID: <u>25184668</u>

Onishi M, Koga T, Hirata A, Nakamura T, Asakawa H, Shimoda C, et al., Fukui Y. 2010. Role of septins in the orientation of forespore membrane extension during sporulation in fission yeast. Mol Cell Biol 30(8): 2057-74. PubMed ID: 20123972

Patterson GH, Knobel SM, Sharif WD, Kain SR, Piston DW. 1997. Use of the green fluorescent protein and its mutants in quantitative fluorescence microscopy. Biophys J 73(5): 2782-90. PubMed ID: <u>9370472</u>

Petit CS, Mehta S, Roberts RH, Gould KL. 2005. Ace2p contributes to fission yeast septin ring assembly by regulating *mid2*⁺ expression. J Cell Sci 118(Pt 24): 5731-42. PubMed ID: <u>16317047</u>

Pollard TD, Wu JQ. 2010. Understanding cytokinesis: lessons from fission yeast. Nat Rev Mol Cell Biol 11(2): 149-55. PubMed ID: 20094054

Prislusky MI, Lam JGT, Contreras VR, Ng M, Chamberlain M, Pathak-Sharma S, et al., Seveau S. 2024. The septin cytoskeleton is required for plasma membrane repair. EMBO Rep 25(9): 3870-3895. PubMed ID: 38969946

Rodal AA, Kozubowski L, Goode BL, Drubin DG, Hartwig JH. 2005. Actin and septin ultrastructures at the budding yeast cell cortex. Mol Biol Cell 16(1): 372-84. PubMed ID: <u>15525671</u>

Rutherford KM, Lera-Ramírez M, Wood V. 2024. PomBase: a global core biodata resource-growth, collaboration, and sustainability. Genetics 227(1): 10.1093/genetics/iyae007. PubMed ID: <u>38376816</u>

Saha S, Pollard TD. 2012. Anillin-related protein Mid1p coordinates the assembly of the cytokinetic contractile ring in fission yeast. Mol Biol Cell 23(20): 3982-92. PubMed ID: <u>22918943</u>

Singh D, Liu Y, Zhu YH, Zhang S, Naegele SM, Wu JQ. 2025. Septins function in exocytosis via physical interactions with the exocyst complex in fission yeast cytokinesis. Elife 13:RP101113. 10.7554/eLife.101113. PubMed ID: 41171630

Sirajuddin M, Farkasovsky M, Hauer F, Kühlmann D, Macara IG, Weyand M, Stark H, Wittinghofer A. 2007. Structural insight into filament formation by mammalian septins. Nature 449(7160): 311-5. PubMed ID: <u>17637674</u>

Sohrmann M, Fankhauser C, Brodbeck C, Simanis V. 1996. The *dmf1/mid1* gene is essential for correct positioning of the division septum in fission yeast. Genes Dev 10(21): 2707-19. PubMed ID: 8946912



Takizawa PA, DeRisi JL, Wilhelm JE, Vale RD. 2000. Plasma membrane compartmentalization in yeast by messenger RNA transport and a septin diffusion barrier. Science 290(5490): 341-4. PubMed ID: <u>11030653</u>

Tasto JJ, Morrell JL, Gould KL. 2003. An anillin homologue, Mid2p, acts during fission yeast cytokinesis to organize the septin ring and promote cell separation. J Cell Biol 160(7): 1093-103. PubMed ID: 12668659

Varela Salgado M, Piatti S. 2024. Septin organization and dynamics for budding yeast cytokinesis. J Fungi (Basel) 10(9): 10.3390/jof10090642. PubMed ID: 39330402

Vrabioiu AM, Mitchison TJ. 2006. Structural insights into yeast septin organization from polarized fluorescence microscopy. Nature 443(7110): 466-9. PubMed ID: <u>17006515</u>

Wang N, Wang M, Zhu YH, Grosel TW, Sun D, Kudryashov DS, Wu JQ. 2015. The Rho-GEF Gef3 interacts with the septin complex and activates the GTPase Rho4 during fission yeast cytokinesis. Mol Biol Cell 26(2): 238-55. PubMed ID: 25411334

Wu JQ, Kuhn JR, Kovar DR, Pollard TD. 2003. Spatial and temporal pathway for assembly and constriction of the contractile ring in fission yeast cytokinesis. Dev Cell 5(5): 723-34. PubMed ID: <u>14602073</u>

Wu JQ, Ye Y, Wang N, Pollard TD, Pringle JR. 2010. Cooperation between the septins and the actomyosin ring and role of a cell-integrity pathway during cell division in fission yeast. Genetics 186(3): 897-915. PubMed ID: 20739711

Ye Y, Zhang S, Gregory JR, Osmani AH, Goodyear EG, Wu JQ. 2025. Roles of the MO25 protein Pmo25 in contractilering stability and localization of the NDR kinase Sid2 during cytokinesis. bioRxiv: pii: 2025.05.13.653815. 10.1101/2025.05.13.653815. PubMed ID: 40463288

Zhang S, Singh D, Zhu YH, Zhang KJ, Melero A, Martin SG, Wu JQ. 2025. The Ync13-Rga7-Rng10 complex selectively coordinates secretory vesicle trafficking and secondary septum formation during cytokinesis. PLoS Biol 23(10): e3003466. PubMed ID: 41144523

Funding: J.R.G is supported by the Cellular, Molecular, and Biochemical Sciences Training Program (T32 GM141955). The work was supported by the National Institute of General Medical Sciences of the National Institutes of Health (grant R01 GM118746 to J.-Q.W.). The content is solely the responsibility of the authors and does not necessarily represent the official views of the National Institutes of Health.

Author Contributions: Jack R. Gregory: conceptualization, formal analysis, funding acquisition, investigation, methodology, visualization, project administration, writing - original draft, writing - review editing. Nicholas J. Ricottilli: investigation, methodology, writing - review editing. Jian-Qiu Wu: conceptualization, supervision, resources, funding acquisition, writing - review editing.

Reviewed By: Anonymous

Nomenclature Validated By: Anonymous

History: Received November 10, 2025 **Revision Received** November 22, 2025 **Accepted** November 24, 2025 **Published Online** November 26, 2025 **Indexed** December 10, 2025

Copyright: © 2025 by the authors. This is an open-access article distributed under the terms of the Creative Commons Attribution 4.0 International (CC BY 4.0) License, which permits unrestricted use, distribution, and reproduction in any medium, provided the original author and source are credited.

Citation: Gregory JR, Ricottilli NJ, Wu JQ. 2025. Localizations of the septin Spn4 tagged with GFP and mEGFP in fission yeast. microPublication Biology. <u>10.17912/micropub.biology.001930</u>